

Voltammetric Behaviors of Chemically Modified Electrodes Based on Zirconium Phosphonate Film

Hun-Gi Hong

Department of Chemistry, Sejong University, Seoul 133-747, Korea

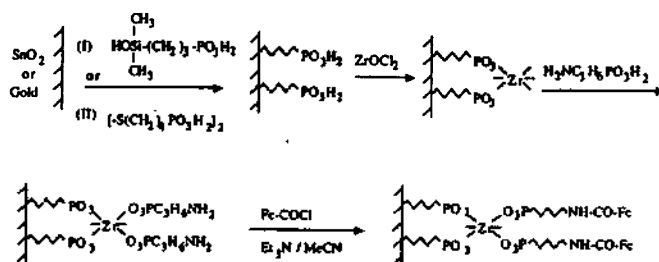
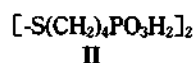
Received March 31, 1995

Electroactive monolayers based on zirconium(IV) phosphonate film were prepared on gold and tin oxide electrodes by sequential layer-by-layer deposition technique. High transfer coefficient values and surface coverages of surface bound redox molecules were obtained from the electrochemical measurements of heterogeneous electron transfer rates for monolayer modified electrodes. 1,10-Decanediybis(phosphonic acid) (DBPA) monolayer as insulating barrier was effective in blocking electron transfer. However, these film modified oxide electrode shows voltammetric behavior of diffusion/permeation process taking place at very small exposed area of modified electrode through channels due to structural defects within film when a very fast redox couple such as $\text{Ru}(\text{NH}_3)_6^{3+}$ is hired.

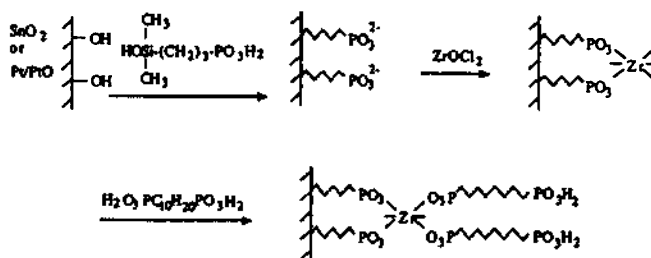
Introduction

The spontaneous self-assembly technique provides a promising strategy for fabricating stable, well-defined monolayer on solid substrates. Monomolecular film of self-assemblies has been used as a model system to understand complex interfacial phenomena such as wetting, adhesion, friction, catalysis and electron/energy transfer on biological membrane. Chemical strategies for self-assembly include mainly thiols,¹⁻⁵ disulfides,⁶ and sulfides⁷ on gold, silanes on silicon dioxide,^{8,9} fatty acids on metal oxide.^{10,11} Another noble strategy for preparation of multilayer has been reported by Mallouk and co-workers.¹² They have found that stable, well-ordered mono/multilayer film based on metal phosphonates can be prepared *via* sequential adsorption technique. Metal phosphonates¹³ are normally made by simple precipitation reaction in which a source of metal ions (II, III, and IV) is mixed with a solution of the appropriate organic phosphonic acids. These metal phosphonate films are thermodynamically stable mechanically robust, and extremely insoluble layered structure.¹³ Since these film are free of pinhole, compact, and electronically insulating, it is interesting to study their property as insulator, spacer and mediator in electron transfer.

In this paper, we report chemical modification of electrode surface by layer-by-layer deposition of small molecule and electrochemical measurements of electron transfer rates of surface bound redox molecules. This sequential deposition technique has two advantages: first, that the thickness and electroactive property of the film can be controlled by choosing the appropriate phosphonic acid chain length and redox molecule; second, that difficulties in synthesis of long chain redox probe can be evaded. In addition, consecutive deposition of small molecule is more effective in decreasing structural defects than one-time deposition of long chain redox molecules. Layer-by-layer deposition is shown in Scheme 1. Building up a redox molecule-terminated film based on metal phosphonate requires first anchoring of molecules bearing the phosphonic acid group through adsorption or covalent binding to the substrate. Two anchoring agents (I and II)



Scheme 1. Ferrocene-modified electrodes by sequential adsorption of APP and 1-Ferrocenoyl chloride.



Scheme 2. Electroinactive DBPA-modified oxide electrodes by sequential adsorption of 3-(hydroxydimethylsilyl)propyl phosphonic acid (HDPA) and Zr(IV).

are used in this work. Electrochemical measurements of these films reveals that redox molecule can be covalently bound on metal phosphonate film structure and that kinetic informations on the electron transfer of the redox couple can be obtained by applying Laviron's theory.¹⁴ Scheme 2 shows adsorption procedure of 1,10-decanediylbis(phosphonic acid) (DBPA) monolayer on zirconium(IV)-terminated metal oxide electrodes. An interesting use of such monolayer film is as insulating barriers at electrode surfaces. For monolayer films sufficiently free from pinhole defects, electron transfer of solution redox species should be effectively blocked from the electrode surface. In this work, it is reported that the heterogeneous electron transfer kinetics of redox couples are slowed at DBPA monolayer-derivatized electrodes.

Experimental

Reagents and materials. Ferrocenecarboxylic acid, zirconyl chloride octahydrate, 1,10-dibromodecane, 1,4-dibromobutane, triethyl phosphite, dicyclohexylcarbodiimide (DCC) and oxalyl chloride were used as received from Aldrich Chemical Co. 3-Aminopropyl phosphonic acid (APP) was purchased from Sigma Chemicals. Ru[(dmbpy)₂(4-methyl-4'-carboxylic acid-2,2'-bipyridine)] (PF₆)₂ (dmbpy=4,4'-dimethyl-2,2'-bipyridine), was obtained from Prof. Thomas E. Mallouk. Methylene chloride and acetonitrile were refluxed over P₂O₅ and distilled before use. Pentane was refluxed over CaCl₂ and distilled. All other chemicals were reagent grade and were used without further purification.

Au thin film electrodes were prepared by sputtering gold onto borosilicate glass slides (1"×3"). The glass was etched first with argon plasma for 30 s and deposited by 1000 Å layer of gold with 50 Å thick layer of chromium underdeposition. Au thin film glass was cut into small pieces (5 mm×15 mm) and used as Au electrode clamped with alligator clip for electric contact. Pt electrodes were made from high purity (99.99%) platinum wire (Johnson-Matthey Co.) and sealed in glass tubing. Platinum electrodes were pretreated by standard anodization¹⁵ for surface oxide formation. SnO₂ electrode was purchased from PPG Industry.

Synthesis. Aqueous solution of 3-(hydroxydimethylsilyl)propyl phosphonic acid (I) were in-situ prepared by reacting 1,3-bis(3-bromopropyl)-1,1,3,3-tetramethyldisiloxane (Huls America), 0.05 mole, with 0.25 mole of P(OC₂H₅)₃ at 150-160 °C for 5 h under nitrogen atmosphere. A 20 mL of concentrated HCl was added and refluxed overnight; addition of 50 mL of 6 N NaOH to the aqueous layer followed by heating at 100 °C for 4 h gave alkaline solution of I. Aliquots of this solution were diluted with water and acidified with HCl just before to use. The disulfide (II) and DBPA were synthesized as reported.¹² 4,4'-Dithiodibutylphosphonic acid (II) was identified by ¹H NMR. ¹H NMR (Bruker AC 200) (DMSO, ppm); 2.6 (t, methylene next to S, 4H); 1.2-1.6 (m, rest of methylenes, 12H). Red microcrystalline ferrocenoyl chloride (Fc-COCl) was obtained from the reaction of ferrocenecarboxylic acid and oxalyl chloride in dried methylene.¹⁶

Instrumentation. Electrochemical measurements were carried out in one-compartment cells with Au thin film electrode, platinum wire and tin oxide as working electrodes, platinum counter electrode, and a saturated calomel electrode (SCE) as a reference electrode. For fast scan voltammetry, an EG & G/ PAR 273A potentiostat was coupled to an IBM personal computer/Digital Oscilloscope (Hitachi 6045) with Model 270 Electrochemical Analysis software (HS program) and RE 0151 X-Y recorder/ HP 7475A X-Y plotter. The electrolyte solutions were prepared with deionized water purified to a resistivity of 18 MΩ/cm with UHQ II system.

Preparation of monolayer on electrodes. The tin oxide electrodes were cleaned by successive ten minutes sonications in Alconox solution, 95% ethanol and deionized water. A 5 mM solution of I was prepared by diluting and acidifying the alkaline stock solution to pH 3 with HCl. Tin oxide and anodized platinum electrodes were immersed and heated to 50 °C for 3 days in this solution. After silanization by I, the oxide electrodes were rinsed with deionized water thoroughly. Monofunctional silanol of I was reacted with free

surface hydroxide of oxide electrode *via* covalent bonding.¹⁷ In case of gold surface, it is well known that bifunctional molecules such as II bind *via* the disulfide group to form compact monolayer.⁶ The gold thin film electrodes were cleaned by sonication in chloroform followed by immersion for 10 s in "piranha" solution (3:1 mixture of concentrated H₂SO₄ and 30% H₂O₂ heated to 100 °C) prior to use. After rinsing with deionized water and drying with nitrogen gas blowing, gold electrodes were immersed in 5 mM ethanol solution of disulfide II for 1 day at room temperature. Upon removal from the deposition solution of II, the gold electrodes were rinsed with fresh ethanol and water. Scheme 1 shows the sequential adsorption procedure used to prepare electroactive monolayers on gold and tin oxide electrode. Tin oxide treated with I and gold treated with II give surface-reactive phosphonic acid at approximately monolayer coverage. The phosphonic acid-modified surface was successively immersed in 5.0 mM zirconyl chloride for 5 h and 5.0 mM 3-aminopropyl phosphonic acid aqueous solution for 15 h according to Scheme 1. After rinsing of amine-surface with 5% Na₂CO₃ solution and deionized water, electrodes were placed *in vacuo* even at 50 °C for 10 h. The dried electrodes were immersed in 2 mM acetonitrile solution of ferrocenoyl chloride for 15 h at room temperature. Finally, ferrocene is covalently linked *via* amide bond on the outer surface of electrode at this stage. The electrodes were removed from the coating solution and washed with fresh ethanol, water, 5% Na₂CO₃ solution and water consecutively. In case of Ruthenium(II) complex, neutral amine-derivatized tin oxide electrode was soaked in 1 mM acetonitrile solution of Ru[(dmbpy)₂(4-methyl-4'-carboxylic acid-2,2'-bipyridine)] (PF₆)₂ for 12 h in the presence of DCC. In the preparation of electroinactive DBPA monolayer on oxide electrodes, zirconium(IV)-terminated oxide electrodes were immersed in 1 mM DBPA aqueous solution for 1 day at room temperature. This procedure is shown in Scheme 2.

Results and Discussion

Cyclic voltammetry was used to characterize electroactive monolayers since it allows for the determination of the quantity of immobilized ferrocene (Γ, in mol/cm² by integration of the voltammetric peak) and redox potential (E^o, taken as the average of the anodic and cathodic peak potentials). Figure 1A shows typical cyclic voltammogram of ferrocene-terminated gold electrode. The anodic and cathodic peaks are quite symmetric and the separation of peak potential (ΔE_p) is *ca.* 60 mV at slow scan rates (20-200 mV/sec). Though ΔE_p is greater than the predicted (0 mV) for an ideal surface wave, it might be due to quasi-reversibility of immobilized ferrocene. The ratio of anodic and cathodic peak current was quite close to unity and these current values are linear to scan rate (shown in Figure 1B). These facts are characteristic to the surface-confined redox molecule.¹⁸ Maximum coverage of ferrocene is 4.5×10⁻¹⁰ mol/cm², which is obtained by treating ferrocene as a sphere of diameter 6.6 Å and by assuming hexagonal close packing.¹⁹ Experimentally observed surface coverage is 5.6×10⁻¹⁰ mol/cm² in this system. However, maximum coverage of ferrocene could be 6.8×10⁻¹⁰ mol/cm² on zirconium phosphonate structure if a ferrocene is occupied with each phosphonate group.

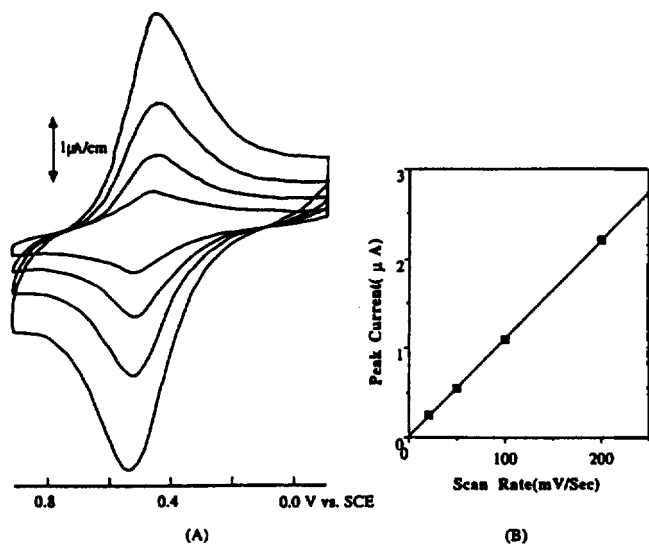


Figure 1. (A) Cyclic voltammograms of ferrocene-modified gold electrode in 0.1 M NaClO₄. Scan rate: 20, 50, 100, 200 mV/sec. (B) Plot of anodic peak currents vs. Scan rate.

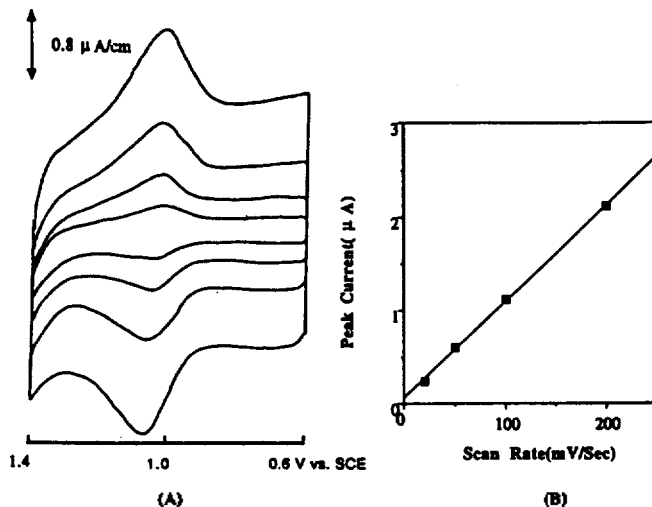


Figure 3. (A) Cyclic voltammograms of Ru[(dmbpy)₂(4-methyl-4'-carboxylic acid-2,2'-bipyridine)](PF₆)₂-modified SnO₂ electrode in 1.0 N H₂SO₄. Scan rate: 20, 50, 100, 200 mV/sec. (B) Plot of anodic peak currents vs. Scan rate.

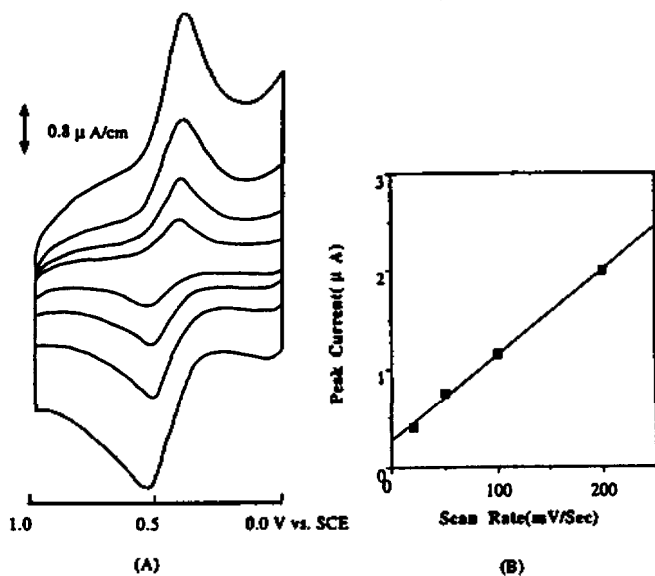


Figure 2. (A) Cyclic voltammograms of ferrocene-modified SnO₂ electrode in 0.1 M NaClO₄. Scan rate: 20, 50, 100, 200 mV/sec. (B) Plot of anodic peak currents vs. Scan rate.

Because each phosphonate group occupies an area of 24 Å², which is reported elsewhere.¹³ Chidsey and coworkers reported a larger coverage of 5.8×10^{-10} mol/cm² for a ferrocene monolayer of longer alkyl chain.²⁰ With this in consideration, it is expected that a few degrees of structural disorder due to dense packing was introduced in this system.

Cyclic voltammogram of ferrocene modified on tin oxide electrode is shown in Figure 2. This shows same voltammetric features of surface confined electroactive moiety as in Figure 1. However, surface coverage of ferrocene was measured to 1.6×10^{-10} mol/cm². This submonolayer coverage often comes from incomplete silanization with surface active

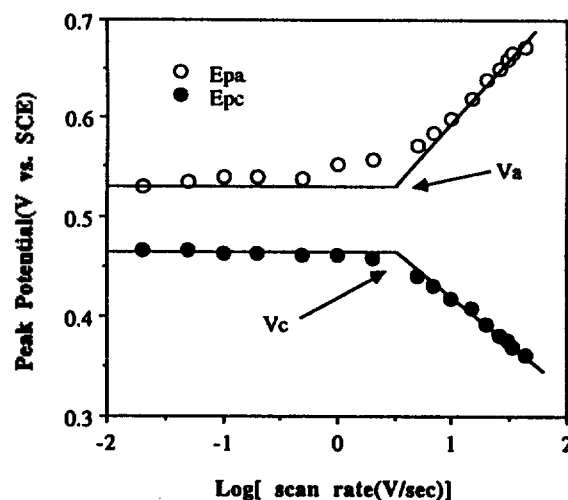


Figure 4. Plot of anodic (E_{pa}) and cathodic (E_{pc}) peak potentials vs. Log (scan rate) for ferrocene-modified gold electrode in 1.0 M NaClO₄. V_a and V_c are anodic and cathodic critical scan rates respectively.

reagent I. In acidic aqueous solution, covalent binding²¹ of monofunctional silanols to the tin oxide competes with dimerization to form the corresponding disiloxane. This fact also explains low coverage value (0.9×10^{-10} mol/cm²) of Ru(II) complex covalently attached to tin oxide electrode *via* amide linkage, according to Scheme 1. This redox couple is spherical and its diameter was estimated to *ca.* 10.2 Å by CPK model.²² Maximum coverage based on CPK model is 2.0×10^{-10} mol/cm². Figure 3A shows well-developed, symmetrical surface waves of Ru(II) redox molecule. Very small value of ΔE_p (10 mV) was obtained for this complex, compared to peak splitting of modified ferrocene. This indicates that immobilized Ru(II) molecules are fairly reversible in charge transfer. Most cyclic voltammograms in this experi-

ment show relatively larger peak-widths at half-height (180–200 mV) than the predicted (90 mV) from theory.¹⁸ This broadening is attributed to variations in local redox couple environments due to differences in binding sites on the surface and interactions between redox molecules.

Figure 4 shows the variations in ΔE_p vs. logarithm of scan rate for a surface-confined ferrocene on gold electrode prepared according to Scheme 1. As the scan rate is increased from 20 to 500 mV/s, this electrode begins to show quasi-reversible behavior. However, peak potential splitting is largely increased to 300 mV at higher scan rate *ca.* 40 V/s and electron transfer between gold electrode and ferrocene becomes totally irreversible. Theory for the manifestation of slow electron transfers of attached electroactive species has been presented by Laviron.¹⁴ According to Laviron's formalism, the kinetic data such as electron transfer coefficient and rate constant may be obtained from variations in the peak splitting with potential scan rate. These kinetic quantities are calculated from equations (1) and (2) under totally irreversible condition, *i.e.*

$$E_{pc} = E_c^{\circ'} - (RT/anF) \ln(RT�^{\circ}/anFV_c) \quad (1)$$

$$E_{pa} = E_a^{\circ'} - (RT/(1-\alpha)nF) \ln(RT�^{\circ}/(1-\alpha)nFV_a) \quad (2)$$

at scan rate where the ΔE_p is ≥ 200 mV. V_c and V_a are critical scan rates which are obtained from extrapolating the linear portion of the E_p vs. $\log V$ plots to the formal cathodic and anodic potentials $E_c^{\circ'}$ and $E_a^{\circ'}$. The latter are the cathodic and anodic peak potentials observed under reversible condition (*i.e.* at slower scan rate) and are 0.47 and 0.53 V vs. SCE respectively. The slopes of the linear portion of the E_p vs. $\log V$ curves are $-2.3RT/anF$ for the cathodic branch and $2.3RT/(1-\alpha)nF$ for the anodic branch. The heterogeneous electron transfer rate constant k° is given by $anFV_c/RT$ for the cathodic process and $(1-\alpha)nFV_a/RT$ for the anodic process. From the slopes of the two branches, the transfer coefficients α and $1-\alpha$ were evaluated as 0.46 and 0.53. These values are close to 0.5, and their sum is almost unity. This fact demonstrates that a highly defect-less structure may be prepared on electrode by layer-by-layer deposition according to Scheme 1. Lane and Hubbard reported very low values (*ca.* 0.20–0.25) of α and $1-\alpha$ for surface bound ferrocene.²³ Finklea and co-workers¹ have shown that these apparently low transfer coefficients are obtained by highly defective film structure, which was inferred from packing model by long chain alkylthiol molecules. Therefore, layer-by-layer deposition of small molecule is much more effective than deposition of long chain molecules to decrease number of "collapsed" sites inside film. The k° values found for the cathodic and anodic processes (56.6 s^{-1} and 65.2 s^{-1} , respectively) are in reasonable agreement with previously reported^{16,22} assuming that the separation between ferrocene and gold electrode is *ca.* 23–24 Å thick. This distance is easily inferred from the difference by two methylene units ($-\text{CH}_2-$) between 4-aminobenzyl phosphonic acid and 3-aminopropyl phosphonic acid. The difference of 1.2 Å in chain length per methylene group is generally known by ellipsometric studies²³ of self-assembled monolayers of alkylthiol molecules.

Scheme 2 shows the procedure used to prepare DBPA monolayer based on zirconium phosphonate of I covalently anchored to oxide electrodes. Since electrochemistry is quite

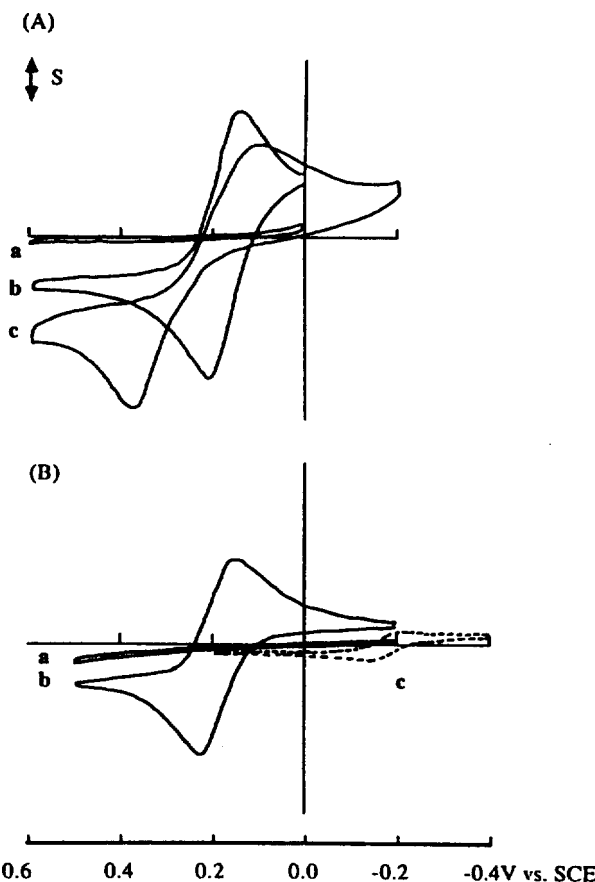


Figure 5. (A) Cyclic voltammograms in aqueous 1 mM $\text{Fe}(\text{CN})_6^{4-}$, 0.1 M NaClO_4 , all scan rates: 50 mV/sec. a) Pt/PtO-I-Zr-DBPA electrode. $S=1 \mu\text{A}/\text{cm}^2$. b) pure Pt electrode. $S=10 \mu\text{A}/\text{cm}^2$. c) Pt/PtO electrode treated with I. $S=1 \mu\text{A}/\text{cm}^2$. (B) Cyclic voltammograms in 1 mM $\text{Fe}(\text{CN})_6^{4-}$, 0.1 M NaClO_4 . All scan rates: 50 mV/sec. a) SnO_2 -I-Zr-DBPA electrode. $S=1 \mu\text{A}/\text{cm}^2$. b) SnO_2 -I electrode. $S=10 \mu\text{A}/\text{cm}^2$. c) SnO_2 -I-Zr-DBPA electrode in 0.1 M NaClO_4 , 1 mM $\text{Ru}(\text{NH}_3)_6^{3+}$. $S=1 \mu\text{A}/\text{cm}^2$.

sensitive to film defects, electrochemical measurements were used to check the structural integrity of the DBPA monolayer adsorbed on electrode. Porter *et al.*² has reported that the rate constant of heterogeneous electron transfer between gold electrode and solution redox couple was greatly reduced on compact surface monolayers of aliphatic thiols. In this work, DBPA monolayer based on phosphonate network should show similar results. Figure 5A shows the cyclic voltammetric current-potential (*i-E*) responses for modified platinum electrodes with 1 mM $\text{Fe}(\text{CN})_6^{4-}$ in 0.1 M NaClO_4 . On bare Pt electrode (b), the formal potential of ferrocyanide is 0.17 V and its voltammogram shows typical reversibility of 60 mV in ΔE_p . The *i-E* response (c) of Pt modified with I still shows quasi-reversibility, which is indicated by extended peak splitting (*ca.* 230 mV). And ferrocyanide oxidation current in (c) was reduced by *ca.* a factor of 10 in comparison with that of (b). This reduction in current indicates that the oxidation of $\text{Fe}(\text{CN})_6^{4-}$ is kinetically limited due to the layer of I as a surface active reagent. Figure 5A-a shows the *i-E* response for a DBPA monolayer on Pt. There is a dramatic difference between the *i-E* responses for $\text{Fe}(\text{CN})_6^{4-}$ at mono-

layer covered and bare Pt electrodes. The observed faradaic current for DBPA monolayer covered electrode is drastically decreased less by a factor of 0.5×10^4 and most of the current is double layer charging current. This indicates that the adsorption of DBPA monolayer on Pt-I-Zr electrode greatly blocks electron transfer and forms impermeable and compact insulating layer on electrode. As shown in Figure 5B-a, this phenomenon is observed again on DBPA modified SnO_2 electrode when the same redox couple is used in solution. Figure 5B-b shows typical cyclic voltammogram obtained from SnO_2 electrode modified with I. However, diffusion-controlled i - E response (Figure 5B-c) is observed on this electrode when the solution-phase redox couple is exchanged to $\text{Ru}(\text{NH}_3)_6^{3+}$. This indicates that redox couple showing very fast heterogeneous electron transfer kinetics is required to study structural defects in DBPA monolayer. The standard rate constant of Ru(III) hexamine is known to be ca. 1 cm/s and one hundred times larger than that of ferrocyanide. The observed small voltammogram clearly shows the characteristics of diffusion process. The solution formal potential (E° , -0.17 V vs. SCE) and peak separation potential (ca. 70 mV) observed on DBPA modified electrode is still equivalent to those on bare Pt electrode. The observed currents on setting near E° of $\text{Ru}(\text{NH}_3)_6^{3+}$ apparently seem to be limiting current which is potential independent. These currents arise from modest permeation²⁴ of DBPA layer by ruthenium(III) hexamine. It is apparent from this discussion that the observed electron transfer takes place by diffusion of redox couple to uncoated electrode surface of very small area. For reversible system,¹⁸ it is possible to assess the uncoated surface area by equation (3):

$$i_p = 2.69 \times 10^5 n^{3/2} A D^{1/2} v^{1/2} C^* \quad (3)$$

where i_p is peak current in ampere, A is the area in cm^2 , D is diffusion coefficient in cm^2/s , v is scan rate in V/s , and C^* is bulk concentration in mol/cm^3 . Solving for A with $i_p = 0.3$ mA and $C^* = 1$ mM, the maximum uncovered area is less than 1.6×10^{-3} cm^2 . This area translates to a fractional uncovered area less than 1.4×10^{-3} for DBPA modified Pt electrode (electrode area is 1.05 cm^2). Unfortunately, the measured current shows variability (ca. 10%) from sample to sample. Such variability most likely is associated with subtle variation in monolayer coverage and degree of organization. Currently, we are investigating heterogeneous electron transfer reaction of redox couples having different size through narrow channels residing in phosphonate monolayer by using rotating disk electrode modified by multilayer of DBPA.

Conclusion

This study demonstrates that a highly defect-less film structure can be prepared on electrode by sequential layer-by-layer deposition through zirconium phosphonate network. High transfer coefficient values and surface coverage were obtained for surface bound ferrocene on gold electrode prepared according to sequential adsorption technique. This sequential deposition procedure also shows diversities in the choice of redox-active probe molecule and supramolecular structure covalently bound on the outer surface of electrode. Electroinactive DBPA monolayer based on metal phospho-

nate shows effectiveness in blocking electron transfer and the amount of defects in this structure can be assessed by electrochemical methods.

Acknowledgment. This work was supported in part by Daeyang Research Foundation, Sejong University, 1993 and by NON DIRECTED RESEARCH FUND, Korea Research Foundation, 1994.

References

- (a) Finklea, H. O.; Robinson, L. R.; Blackburn, A.; Richter, B.; Allara, D. L.; Bright, T. *Langmuir* **1986**, *2*, 239. (b) Finklea, H. O.; Avery, S.; Lynch, M.; Furtch, T. *Langmuir* **1987**, *3*, 409.
- Porter, M. D.; Bright, T. B.; Allara, D. L.; Chidsey, C. E. D. *J. Am. Chem. Soc.* **1987**, *109*, 3559.
- (a) Miller, C.; Cuendet, P.; Gratzel, M. *J. Phys. Chem.* **1991**, *95*, 877. (b) Miller, C.; Gratzel, M. *J. Phys. Chem.* **1991**, *95*, 5225.
- (a) Bain, C. D.; Whitesides, G. M. *J. Am. Chem. Soc.* **1988**, *110*, 3665. (b) Bain, C. D.; Whitesides, G. M. *J. Am. Chem. Soc.* **1988**, *110*, 5897. (c) Bain, C. D.; Whitesides, G. M. *J. Am. Chem. Soc.* **1988**, *110*, 6560. (d) Wasserman, S. R.; Whitesides, G. M.; Tidswell, I. M.; Ocko, B. M.; Pershan, P. S.; Axe, J. D. *J. Am. Chem. Soc.* **1989**, *111*, 5852 and references therein.
- Nuzzo, R. G.; Dubois, L. H.; Allara, D. L. *J. Am. Chem. Soc.* **1990**, *112*, 558.
- (a) Nuzzo, R. G.; Allara, D. L. *J. Am. Chem. Soc.* **1983**, *105*, 4481. (b) Nuzzo, R. G.; Zegarski, B. R.; Dubois, L. H. *J. Am. Chem. Soc.* **1987**, *109*, 733. (c) Nuzzo, R. G.; Fusco, F. A.; Allara, D. L. *J. Am. Chem. Soc.* **1987**, *109*, 2358.
- Troughton, E. B.; Bain, C. D.; Whitesides, G. M.; Nuzzo, R. G.; Allara, D. L.; Porter, M. D. *Langmuir* **1988**, *4*, 365.
- Sagiv, J. *J. Am. Chem. Soc.* **1980**, *102*, 92.
- (a) Maoz, R.; Sagiv, J. *J. Colloid Interface Sci.* **1984**, *100*, 465. (b) Wasserman, S. R.; Tao, Y.-T.; Whitesides, G. M. *Langmuir* **1989**, *5*, 1074. (c) Tillman, N.; Ulman, A.; Schildkraut, J. S.; Penner, T. L. *J. Am. Chem. Soc.* **1988**, *110*, 6136. (d) Maoz, R.; Sagiv, J. *Langmuir* **1987**, *3*, pp 1034-1051.
- (a) Allara, D. L.; Nuzzo, R. G. *Langmuir* **1985**, *1*, 45. (b) Allara, D. L.; Nuzzo, R. G. *Langmuir* **1985**, *1*, 52.
- Schlotter, N. E.; Porter, M. D.; Bright, T. B.; Allara, D. L. *Chem. Phys. Lett.* **1986**, *132*, 93.
- (a) Lee, H.; Kepley, L. R.; Hong, H.-G.; Mallouk, T. E. *J. Am. Chem. Soc.* **1988**, *110*, 618. (b) Lee, H.; Kepley, L. R.; Hong, H.-G.; Akhter, S.; Mallouk, T. E. *J. Phys. Chem.* **1988**, *92*, 2597. (c) Akhter, S.; Lee, H.; Kepley, L. R.; Hong, H.-G.; Mallouk, T. E.; White, J. M. *J. Vac. Sci. Technol. A* **1989**, *7*, 1608. (d) Cao, G.; Hong, H.-G.; Mallouk, T. E. *Acc. Chem. Res.* **1992**, *25*, 420.
- (a) Dines, M. B.; DiGiacomo, P. *Inorg. Chem.* **1981**, *20*, 92; (b) Dines, M. B.; DiGiacomo, P.; Callahan, K. P.; Griffith, P. C.; Lane, R.; Cooksey, R. E. in *Chemically Modified Surfaces in Catalysis and Electrocatalysis*; J. Miller, Ed. (ACS Symp. Ser. 192, 1982), p 223; (c) Dines, M. B.; Cooksey, R. E.; Griffith, P. C. *Inorg. Chem.* **1983**, *22*, 1003 (d) Clearfield, A.; Smith, G. D. *Inorg. Chem.*

- 1969, 8, 431 (e) Cao, G.; Lynch, V. M.; Swinnea, J. S.; Mallouk, T. E. *Inorg. Chem.* **1990**, 29, 2112.
14. Laviron, E. *J. Electroanal. Chem.* **1979**, 101, 19.
15. Lenhard, J. R.; Murray, R. W. *J. Am. Chem. Soc.* **1978**, 100, 7870.
16. Hong, H.-G.; Mallouk, T. E. *Langmuir* **1991**, 7, 2362.
17. Murray, R. W. In *Electroanalytical Chemistry*; Bard, A. J., Ed.; Marcel Dekker: New York, 1984; Vol. 13, p 191.
18. Bard, A. J.; Faulkner, L. R. *Electrochemical Methods: Fundamentals and applications*; Wiley: New York, 1980.
19. Seiler, P.; Dunitz, J. D. *Acta Cryst., Sect. B* **1979**, B35, 1068.
20. Chidsey, C. E. D.; Bertozzi, C. R.; Putvinski, T. M.; Mujscce, A. M. *J. Am. Chem. Soc.* **1990**, 112, 4301.
21. Haller, I. *J. Am. Chem. Soc.* **1978**, 100, 8050.
22. Finklea, H. O.; Hanshew, D. D. *J. Am. Chem. Soc.* **1992**, 114, 3173.
23. Lane, R. F.; Hubbard, A. T. *J. Phys. Chem.* **1973**, 77, 1401.
24. Ikeda, T.; Schmehl, R.; Denisevich, P.; Willman, K.; Murray, R. W. *J. Am. Chem. Soc.* **1982**, 104, 2683.